Available online at www.sciencedirect.com
ScienceDirect
Proceedings of the Combustion Institute (2022) 1–9
Proceedings of the Combustion Institute
www.elsevier.com/locate/proci

Atomistic insight into enhanced thermal decomposition of energetic material on graphene oxide

Muye Feng [a], Yi Wang [a], Kai H. Luo [b,*]

[a] Center for Combustion Energy, Key Laboratory of Thermal Science and Power Engineering of Ministry of Education, Department of Energy and Power Engineering, Tsinghua University, Beijing 100084, China
[b] Department of Mechanical Engineering, University College London, Torrington Place, London WC1E 7JE, UK

Received 3 January 2022; accepted 6 July 2022

Abstract

Graphene oxide (GO)-based nanocomposites are promising additives for practical applications of cyclotrimethylenetrinitramine (RDX). GO is not only an excellent support for nanoparticles, but also has independent catalytic activities, which have not been well understood. In this study, the reactive molecular dynamics simulation method is employed to investigate the kinetics and fundamental catalytic mechanisms of the thermal decomposition of RDX on GO. The RDX decomposition reaction is found to be enhanced in the presence of GO and the catalytic effect is better at low than at high temperatures. Additionally, GO addition lowers the activation energy by 11.35% compared with the thermal decomposition of pure RDX. The study shows that the catalytic capabilities of GO primarily originate from its functional groups that promote both the initiation and intermediate reactions. Furthermore, the H exchange process between the functional groups on GO and RDX/RDX intermediates plays an important role in the reaction. GO is further oxidized with more functional groups during the reaction, which are also involved in the catalytic activities. Finally, the energy barrier of functional group-participated reactions is found to be lower than their corresponding unimolecular decomposition leading to enhanced thermal decomposition of RDX. The proposed catalytic mechanisms in the present research should also be applicable to other energetic materials of the same class with a similar structure as RDX.

Keywords: RDX; Graphene oxide; Thermal decomposition; Molecular dynamics; Reactive force field

1. Introduction

Cyclotrimethylenetrinitramine (RDX, $C_3H_6O_6N_6$) is one of the most widely used energetic materials formulated in composite solid propellants and applied in both military and industrial fields [1]. The thermal decomposition of RDX received worldwide attention in the past decades as it significantly affects the combustion performance of propellants [2]. In order to improve the decomposition and subsequent combustion of RDX, a common strategy is to add nano-sized energetic

* Corresponding author.
E-mail address: k.luo@ucl.ac.uk (K.H. Luo).

https://doi.org/10.1016/j.proci.2022.07.047

additives due to their large specific surface areas and excellent catalytic effects. Instead of the conventional metal/metal oxide compound catalysts, graphene oxide (GO)-based nanocomposites have attracted increasing attention as novel additives for RDX, which can suppress the aggregation of nanoparticles and further enhance the catalytic performance [2–9]. Additionally, GO is exothermic and energetically involved in the combustion process releasing extra energy owing to its functional groups [10].

He et al. [2] studied the catalytic reactivity of GO stabilized transition metal complexes of triaminoguanidine on RDX thermolysis. They observed a reduction in activation energy and an increase in heat release. An et al. [3] evaluated the catalytic combustion of RDX-based propellants with Cu_2O-PbO/GO and CuO-Bi_2O_3/GO nanocomposites. It was reported that the burning rate was remarkably enhanced and the plateau combustion was achieved, which is important for practical applications. The thermal decomposition of RDX on NGO (nitrated GO) [4], Cu-Co/GO [5], $CuFe_2O_4$/GO [6], Bi_2WO_6/GO [7], $MgWO_4$/GO [8] and $MgFe_2O_4$/GO [9] was investigated in a similar way. The results from these studies all showed different levels of decrease in both thermal decomposition temperature and activation energy. The successful preparation of these nanocomposites and their corresponding promising test results demonstrate the potential of GO-based materials for practical RDX applications.

Experimental studies focused more on the preparation and characterization of GO-based nanocomposites, and their effects on the performance of thermal decomposition and combustion of RDX, leaving detailed mechanisms to intuition and empirical analysis. In addition to the prevention of nanoparticle aggregation, a better catalytic performance of GO-based nanocomposites than their monocomponents (separate metal-based and GO counterparts) was demonstrated and attributed to the generic "synergistic effect" [3,6–8]. No plausible mechanisms have been proposed so far for the independent catalytic activity of GO on the thermal decomposition of RDX, but such mechanisms are highly desirable and of great practical significance in helping the design, preparation and application of GO-based nanocomposites for energetic materials. In this study, reactive molecular dynamics simulations are performed to investigate the kinetics and fundamental catalytic mechanisms of the thermal decomposition of RDX on GO. The energy barriers for key and representative catalytic reactions are also calculated to provide a deeper insight into the enhancement resulting from GO. Finally, the catalytic effects of GO on the thermal decomposition of RDX are revealed.

2. Methods

2.1. ReaxFF reactive force field molecular dynamics simulation

The ReaxFF reactive force field molecular dynamics (MD) simulation method is based on the bond-order concept and capable of modelling dissociation, transition and formation of chemical bonds, which is therefore applicable to describe reactive systems. Force field parameters are trained against quantum mechanics (QM) calculations or/and experimental data. Compared with QM, ReaxFF MD is computationally much cheaper but reproduces a comparable level of accuracy. In the meantime, ReaxFF is superior to the classic MD, as the latter is incapable of simulating chemical reactions. Hence, ReaxFF MD is a powerful method for studying long-time large-scale reactive systems that are impractical or impossible for QM or classic MD methods. ReaxFF bond orders are calculated from interatomic distances directly as in Eq. (1) and continually updated at every time step thereby enabling connectivity changes [11].

$$\begin{aligned} BO_{ij} = BO_{ij}^{\sigma} + BO_{ij}^{\pi} + BO_{ij}^{\pi\pi} = \exp\left[p_{bo1}\left(r_{ij}/r_o^{\sigma}\right)^{p_{bo2}}\right] \\ + \exp\left[p_{bo3}\left(r_{ij}/r_o^{\pi}\right)^{p_{bo4}}\right] + \exp\left[p_{bo5}\left(r_{ij}/r_o^{\pi\pi}\right)^{p_{bo6}}\right] \end{aligned} \tag{1}$$

where BO is the bond order between atoms i and j, r_{ij} is interatomic distance, r_o terms are equilibrium bond lengths, and p_{bo} terms are empirical parameters. Equation (2) shows the general expression of energy components contributing to the ReaxFF potential [12].

$$\begin{aligned} E_{\text{system}} = E_{\text{bond}} + E_{\text{over}} + E_{\text{under}} + E_{\text{lp}} + E_{\text{val}} \\ + E_{\text{tor}} + E_{\text{vdWaals}} + E_{\text{Coulomb}} \end{aligned} \tag{2}$$

where E_{system}, E_{bond}, E_{over}, E_{under}, E_{lp}, E_{val}, E_{tor}, E_{vdWaals} and E_{Coulomb} represent total energy, bond energy, overcoordination energy penalty, undercoordination stability, lone pair energy, valence angle energy, torsion angle energy, van der Waals energy and Coulomb energy, respectively.

More information on the ReaxFF formulation and development is provided in references [11,12]. ReaxFF MD has proven its efficiency and capability for investigating a wide range of catalytic and combustion systems [13–18].

2.2. Simulation details

All of the ReaxFF MD simulations are performed using the LAMMPS package [19]. The ReaxFF-*lg* description [20], which has proven to be able to accurately predict chemical reactions of energetic materials including RDX and their interactions with graphene-based materials [21,22], is chosen as a suitable force field for the present

Please cite this article as: M. Feng, Y. Wang and K.H. Luo, Atomistic insight into enhanced thermal decomposition of energetic material on graphene oxide, Proceedings of the Combustion Institute, https://doi.org/10.1016/j.proci.2022.07.047

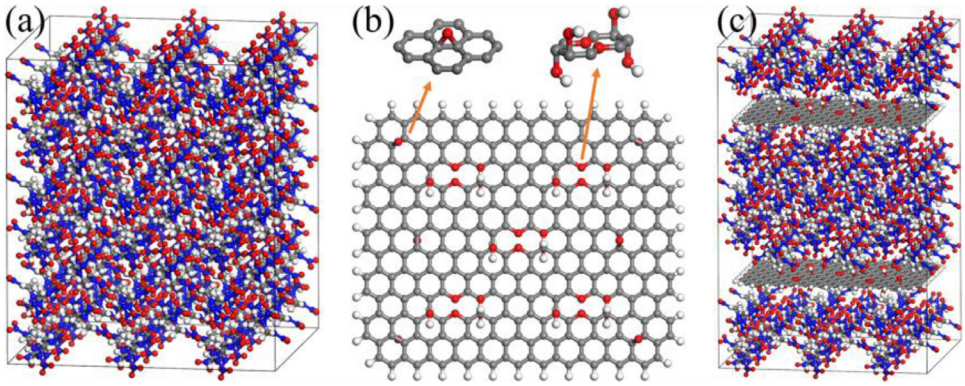

Fig. 1. Configuration of the simulation systems: (a) pure RDX, (b) GO structure, and (c) RDX/GO composite. C, H, O and N atoms are represented in grey, white, red and blue, respectively.

study. In order to correctly describe the fast chemistry of RDX, a time step of 0.1 fs is used for all of the simulations. The results are outputted every 0.1 ps. A commonly used 0.3 bond order cutoff is adopted for obtaining the species information throughout the simulation. The visualization of simulation results is rendered by OVITO [23].

The most stable α-RDX morphology is employed and the crystal structure is obtained from Ref. [24] with lattice parameters of $a = 11.6103$ Å, $b = 10.7291$ Å, and $c = 13.2013$ Å. Two periodic simulation systems are built to study the catalytic effect of GO on the thermal decomposition of RDX. A $3 \times 3 \times 3$ supercell containing 216 RDX molecules is constructed as the base system (Fig. 1a). The RDX/GO composite system includes two functionalized GO sheets uniformly inserted into the base system along the c direction (Fig. 1c). Fig. 1b shows the detailed structure of GO ($C_{286}H_{66}O_{36}$), which is modified based on a pristine graphene sheet. There are two types of functional groups on the GO: (1) a simple epoxy group [25]; (2) a divacancy decorated by two ethers with four additional OH groups attached to the nearby C atoms [26]; the number of them are six and five, respectively. The edge C atoms of the graphene sheet are adjusted with H atoms.

After energy minimization, both systems are equilibrated under the isothermal-isobaric (NPT) ensemble at 300 K and 0 pressure for 50 ps to relax the residual stress. For the composite system, the NPT procedure also eliminates the redundant vacuum space in the artificially constructed model. The equilibrated lattice parameters of the $3 \times 3 \times 3$ RDX supercell are $a = 34.3469$ Å, $b = 31.7401$ Å, and $c = 39.0536$ Å, which agree well with the above experimental values [24] based on the unit cell. Similarly, the density after equilibration is 1.87 g/cm^3 and very close to the normal density. The equilibrated composite system has lattice parameters of $a = 33.0220$ Å, $b = 30.5157$ Å, and $c = 50.8200$ Å with a density of 1.82 g/cm^3. The time evolution of relative potential energy and density of the two systems is given in Fig. S1 in Supplementary Material I, demonstrating that 50 ps is enough for relaxation. These two equilibrated systems are finally used to carry out canonical (NVT) ensemble simulations for 100 ps from 1100 to 1600 K with an interval of 100 K. Every simulation case (one system at one temperature) is run three times independently and the results are averaged for analysis.

3. Results and discussion

3.1. Global effects of GO on thermal decomposition of RDX

The thermal decomposition of RDX has been extensively studied by both experimental [27,28] and computational [29,30] methods. Especially, the ReaxFF MD has proven to be an effective technique for investigating the mechanisms and kinetics of catalytic and thermal decomposition of RDX [31–34]. Consistent with these previous works, important reaction pathways such as N-NO_2 homolytic cleavage and HONO elimination, as well as key species including N_2, NO, NO_2, CO, CO_2 and H_2O, are all observed during the thermal decomposition of RDX in the present study, which demonstrates the validity of the obtained results. For the purpose of the present research, the effects of GO addition rather than the pure RDX thermal decomposition are the focus of analysis throughout.

The time evolution of the number of RDX molecules during the thermal decomposition over a temperature range from 1100 to 1600 K is used to investigate the difference in reaction rate between RDX and RDX/GO systems. As can be seen in Fig. 2a, overall, the RDX reaction is accelerated with the rising temperature in both systems. In ad-

Please cite this article as: M. Feng, Y. Wang and K.H. Luo, Atomistic insight into enhanced thermal decomposition of energetic material on graphene oxide, Proceedings of the Combustion Institute, https://doi.org/10.1016/j.proci.2022.07.047

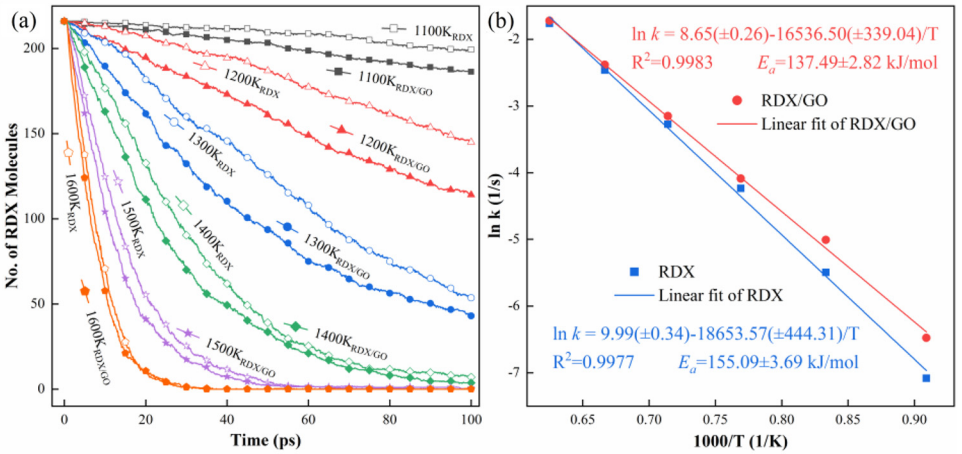

Fig. 2. (a) Time evolution of the number of RDX molecules during the thermal decomposition of RDX and RDX/GO at temperatures ranging from 1100 to 1600 K with an increment of 100 K (uncertainties and errors are shown in Fig. S2 in Supplementary Material I, which demonstrate that the relative evolution trend between RDX and RDX/GO simulation cases is not affected, thereby ensuring the quality of the results); (b) Arrhenius plot and the determination of activation energy for the thermal decomposition of RDX and RDX/GO.

dition, the consumption of RDX is faster in the system of RDX/GO than of RDX at each studied temperature, which indicates the enhancement of the reaction with GO addition. This enhancement was also observed in experimental studies [6–8]. However, as the temperature increases, the difference in reaction rate between the two systems is becoming smaller. At 1600 K, the two lines nearly overlap with each other after about 18 ps. This suggests that the catalytic effect of GO is impaired by the elevated temperature. In other words, GO has a better catalytic performance at low than at high temperatures.

To further quantify the results, the kinetics of the two systems is studied. The thermal decomposition of energetic materials including RDX generally follows the first-order kinetics [31,35], it is therefore employed to evaluate the rate constant k at each studied temperature. Specifically, k can be obtained from the slope of the linear fit of $\ln([RDX]_t/[RDX]_0)$ versus time, where $[RDX]_0$ and $[RDX]_t$ are the RDX concentration at $t = 0$ and any arbitrary moment, respectively. In conjunction with the Arrhenius Equation (Eq. (3)), the activation energy E_a can be determined for the two systems.

$$\ln k = \ln A - (E_a/R) \cdot (1/T) \tag{3}$$

where k, A, E_a, R and T represent rate constant, pre-exponential factor, activation energy, gas constant and absolute temperature, respectively. Fig. 2b shows the Arrhenius plot with the calculation of E_a from the fitting formula. Consistent with the results of Fig. 2a, the gap between ln k of the two systems narrows down with the elevated temperature. At 1600 K, the two ln k values are extremely close to each other, which indicates diminishing catalytic performance of GO at such a high temperature. Based on the kinetic results in Fig. 2, it can be deduced that the enhancement of thermal decomposition of RDX resulting from GO could be negligible if the temperature is higher than 1600 K. The obtained E_a for RDX and RDX/GO is 155.09 and 137.49 kJ/mol, respectively. In the presence of GO, E_a is reduced by 11.35% compared with pure RDX, demonstrating that GO promotes RDX reactions. E_a of pure RDX decomposition reported from experiments varies from 103 to 272 kJ/mol as summarized in a previous study [31], and the experimentally derived E_a of RDX/GO is 122 [7] and 131 kJ/mol [36]. The discrepancy in E_a between the present research and experiments is generally acceptable as a result of the various different conditions adopted including temperature, particle size, structure and loading of GO, calculation methods as well as uncertainties and errors in both the computational and experimental studies. For example, E_a of RDX/GO is overestimated in the present research in comparison with Zhang et al.'s [7] experiment, which can be attributed to the different GO loadings (mass ratio of GO and RDX is 1:5.89 and 1:4, respectively). Therefore, E_a values in the present research can be considered to be in good agreement with the experimental results.

It is worth mentioning that the simulation results are sensitive to the various conditions mentioned above. In addition to temperature, which has been studied in detail in the present study, the particle size, structure, and GO loading may also affect the results. Generally, smaller particles lead to higher reactivity thus better catalytic effects. A higher GO loading within a specific range

Please cite this article as: M. Feng, Y. Wang and K.H. Luo, Atomistic insight into enhanced thermal decomposition of energetic material on graphene oxide, Proceedings of the Combustion Institute, https://doi.org/10.1016/j.proci.2022.07.047

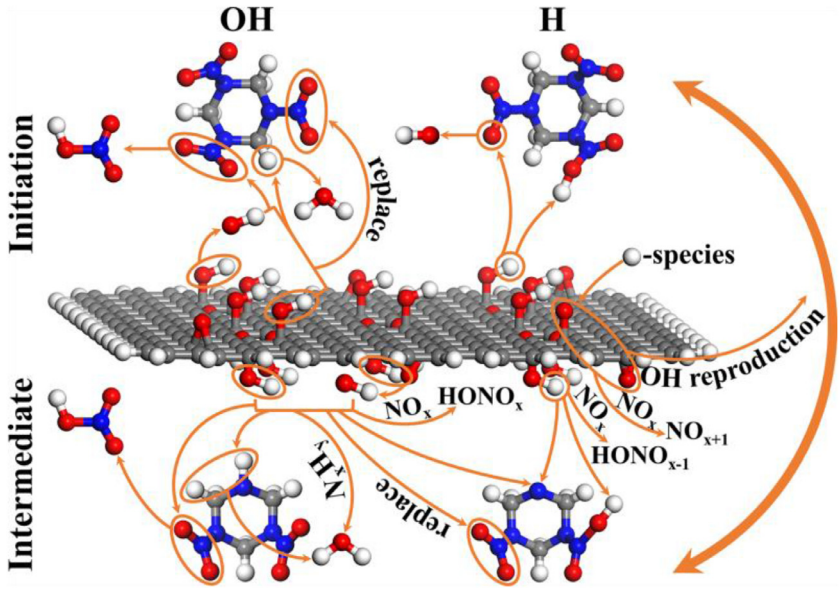

Fig. 3. Major catalytic mechanisms for the thermal decomposition of RDX on GO. The upper and lower halves describe the initiation and intermediate reactions, respectively. The left and right halves describe the OH- and H-related reactions, respectively. The species shown in the lower half are representative RDX intermediates for demonstration.

could result in better catalytic effects but there should be a limit. The effects of GO structure could be complicated. In brief, the detailed trends and mechanisms under various conditions need further studies.

3.2. Catalytic mechanisms of thermal decomposition of RDX with GO

The effects of GO on the thermal decomposition of RDX and associated catalytic activities are further scrutinized. The catalytic mechanisms are sophisticated on the whole due to the complex structure of RDX leading to a variety of intermediates. As a result, the major and pivotal catalytic mechanisms are proposed in the present study via the simultaneous analysis of atomic trajectories and species evolution, as seen in Fig. 3.

The catalytic activities of GO are found to primarily originate from its OH and O functional groups. Specifically, OH both initiates the RDX decomposition and participates in various intermediate reactions. In regard to initiation reactions, OH on GO can directly react with NO_2 or one H of CH_2 on RDX, forming $HONO_2$ and H_2O, respectively. Alternatively, OH can replace the NO_2 with O bonding to the ring N on RDX. In addition to the direct reactions of OH on GO with RDX, OH may leave the GO sheet first and then proceeds with the same reactions. Besides, H of OH on GO is also involved in the initiation reactions. This H is attracted by one O of NO_2 on RDX and attached to the O, after which the formed OH unit either remains on RDX or leaves as a free radical. The O of the epoxy group is not active in the initiation of RDX but takes part in intermediate reactions.

The activity of functional groups in intermediate reactions is more diverse. Similar to initiation reactions, OH is involved in both GO bonded and free radical forms. It reacts with ring RDX intermediates containing N-NO_2, N-H or CH_2 to produce $HONO_2$ or H_2O. Also, it replaces a NO_2 on ring intermediates or directly bonds to a bare ring N which loses its NO_2. Other small species including NO_x and N_xH_y interact with OH as well generating $HONO_x$ and H_2O. Except for the observation that H of OH on GO is adsorbed on O of NO_2 or bare ring N on RDX intermediates, its reaction with NO_x to form $HONO_{x-1}$ is also significant. Additionally, the H further reacts with $HONO_x$ producing H_2O. Based on these findings, H_2O, $HONO_2$, HONO and HON are key species during the catalytic thermal decomposition of RDX on GO, the production of which over time in the two systems is shown in Fig. S3 in Supplementary Material I. The number of these four species is generally larger in the presence of GO, especially at low temperatures where GO has a better catalytic performance. After losing H, the remaining O of OH on GO continues to participate in intermediate reactions if it is not kept to the end of the simulation. The situation of O of the epoxy group is similar. N of NO or NO_2 can connect with O and finally leave the GO sheet as NO_2 or NO_3. Importantly, the interesting H exchange process involving O on GO between the

Please cite this article as: M. Feng, Y. Wang and K.H. Luo, Atomistic insight into enhanced thermal decomposition of energetic material on graphene oxide, Proceedings of the Combustion Institute, https://doi.org/10.1016/j.proci.2022.07.047

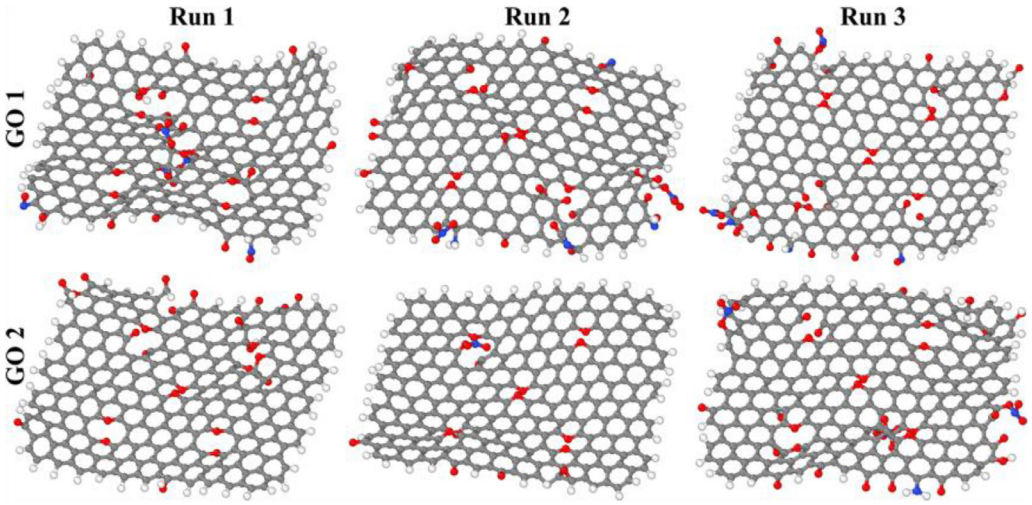

Fig. 4. Structure of GO sheets at the end of the simulations at 1600 K. Results from all of the three independent runs are shown.

functional groups and RDX/RDX intermediates is discovered. To be specific, H of OH on GO is first consumed as described above. Subsequently, the hanging O adsorbs another H from H-containing species leading to the reproduction of OH. Afterwards, this OH undergoes the same catalytic process. An animation demonstrating an example of the H exchange process is provided in Supplementary Material II. According to the mechanisms, it is suggested that the functional groups on GO mainly interact with N- rather than C-species, which could be attributed to the ready availability of N and high reactivity of nitros on RDX. However, the reaction of the functional groups with hydrocarbon radicals could also be expected if the number of functional groups is increased and the simulation time is extended.

The GO structures are monitored throughout the simulations and Fig. 4 illustrates the structure of GO sheets at the end of the simulations at 1600 K. It can be seen that there is no destruction of the structure and all of the sheets are retained well. The functional groups are diminished, however, the GO is further oxidized, especially at the edge of the sheet, mounting more functional groups including O, OH, NO and NH_2. These regenerated functional groups also take part in the reactions facilitating the interatomic exchange. It is noteworthy that some NO_2 radicals are found to adhere to O on GO because of the active interactions between N-species and GO.

Based on the above analysis, the introduction of GO forms a catalytic cycle driven by its functional groups. Specifically, to start with, OH first initiates the decomposition of RDX by reacting with its NO_2 or CH_2 groups. Then, OH also takes part in intermediate reactions involving ring RDX intermediates and other small species. It is important that the reaction of both O of OH (after losing H) and O of the epoxy group on GO with H-containing species can reproduce OH, which subsequently repeats the catalytic process. As a result, the production of H_2O, $HONO_2$, HONO and HON as the key species is increased during the catalytic thermal decomposition. Meanwhile, more functional groups are generated due to further oxidation of GO. Therefore, the interatomic exchange and GO oxidation together drive the catalytic cycle and enhance the decomposition of RDX.

3.3. Energy barrier for key initiation reactions

The nudged elastic band (NEB) method [37] embedded in LAMMPS is used to calculate the energy barrier for the key initiation reactions. The initial and final structures of each reaction are fully relaxed and three intermediate replicas are inserted in between. An illustration of the studied reactions and the corresponding energy barriers are displayed in Fig. 5. Compared with the three unimolecular decomposition pathways of RDX (a1, b1 and c1 in Fig. 5), their initiations by OH or H of OH on GO (a2, b2 and c2 in Fig. 5) all occur at a lower energy barrier, the reduction of which is 91.04%, 64.28% and 29.44%, respectively. Particularly, the energy barriers of the reactions of H and NO_2 on RDX with OH on GO are significantly lower than their unimolecular decomposition, demonstrating the importance of OH functional groups in the catalytic thermal decomposition of RDX on GO. The dissociation energy of C-H and N-NO_2 bonds of RDX from ab initio computations is 355.64 and 175.73 kJ/mol [38], respectively, which shows good agreement and prove

Please cite this article as: M. Feng, Y. Wang and K.H. Luo, Atomistic insight into enhanced thermal decomposition of energetic material on graphene oxide, Proceedings of the Combustion Institute, https://doi.org/10.1016/j.proci.2022.07.047

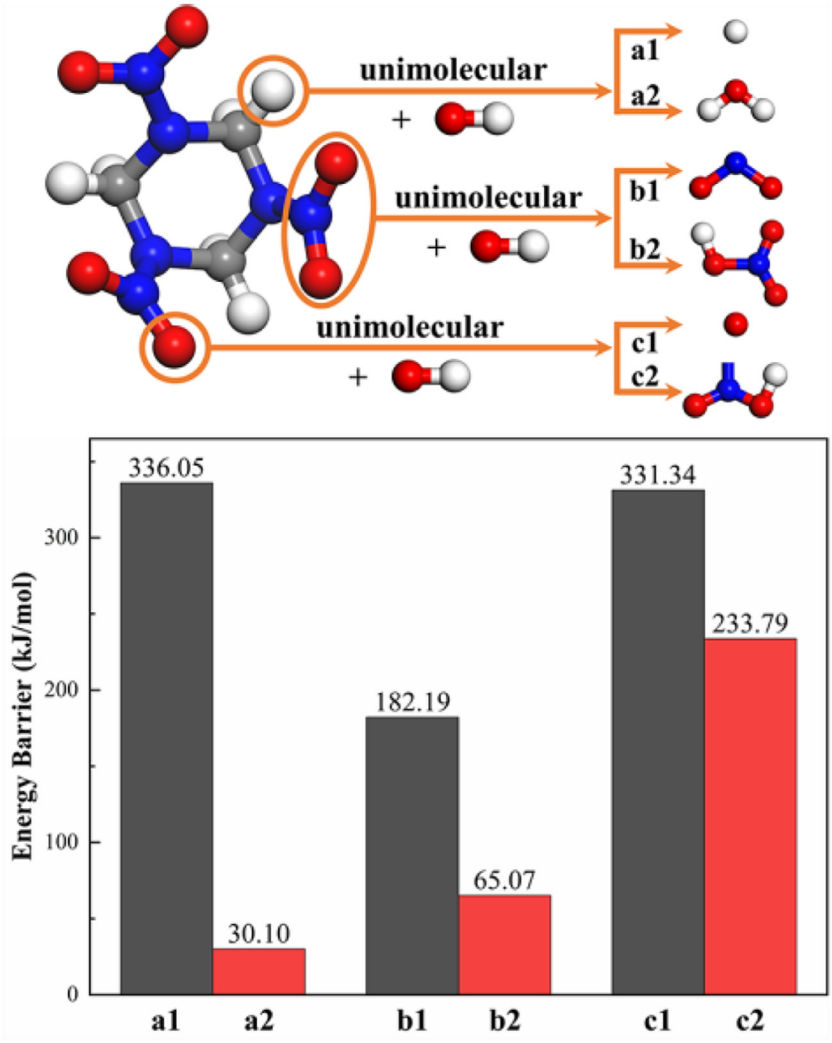

Fig. 5. Energy barrier for key initiation reactions: (a1) unimolecular decomposition forming H, (a2) reaction with OH forming H_2O, (b1) unimolecular decomposition forming NO_2, (b2) reaction with OH forming $HONO_2$, (c1) unimolecular decomposition forming O, and (c2) reaction with H of OH adsorbing the H on O of NO_2.

the effectiveness of the results in the present study. Other similar intermediate reactions should have comparable energy barrier results. Therefore, the functional groups on GO reduce the energy barrier of RDX decomposition reactions thereby enhancing the thermal decomposition of RDX.

4. Conclusions

The kinetics and fundamental catalytic mechanisms of the thermal decomposition of RDX on GO are investigated via ReaxFF MD simulations. The results indicate that the RDX decomposition reaction is enhanced in the presence of GO and the catalytic effect is better at low than at high temperatures. In addition, compared with the thermal decomposition of pure RDX, the addition of GO lowers the activation energy by 11.35%. It is found that the catalytic capabilities of GO primarily originate from its functional groups, which both initiate the RDX decomposition and participate in various intermediate reactions thereby promoting the thermal decomposition of RDX. Furthermore, the H exchange process between the functional groups on GO and RDX/RDX intermediates is observed to facilitate the interatomic reactions. The original functional groups are diminished during the reaction but GO is further oxidized mounting more functional groups mostly at the edge of the sheet, which are also involved in the decomposition reactions. Moreover, all of the GO sheet structures are

Please cite this article as: M. Feng, Y. Wang and K.H. Luo, Atomistic insight into enhanced thermal decomposition of energetic material on graphene oxide, Proceedings of the Combustion Institute, https://doi.org/10.1016/j.proci.2022.07.047

retained well throughout the simulations. Based on the catalytic mechanisms, the energy barriers for key and representative catalytic reactions are calculated. The results show a lower energy barrier for reactions initiated by the functional groups with respect to their corresponding unimolecular decomposition, which leads to the enhanced thermal decomposition of RDX. With the help of molecular dynamics simulations, the catalytic mechanisms of GO-assisted thermal decomposition of RDX are revealed and explained at the atomic level, which are not accessible by the existing experimental techniques, and are therefore a valuable supplement to current experimental results. The findings from the present research could benefit the design of GO-based nanocomposites as additives for RDX. For example, higher catalytic effects would be expected if GO is functionalized with more O-containing groups. The proposed catalytic mechanisms should also be applicable to those energetic materials having a similar structure as RDX, including HMX, TNT and TATB.

It should be noted that due to the complex structure of RDX and limited time scale of MD simulations, the focus of analysis of catalytic mechanisms is on the initial stage of RDX thermal decomposition. The catalytic activity of GO might change at a later stage of the reaction, which needs to be clarified in further studies. Additionally, the behaviors of other functional groups such as carboxyl and the effects of relative loading of different functional groups are also worth exploring in future work.

Declaration of Competing Interest

The authors declare that they have no known competing financial interests or personal relationships that could have appeared to influence the work reported in this paper.

Acknowledgements

Funding from the National Natural Science Foundation of China (Grant No. 52106164), the China Postdoctoral Science Foundation (Grant No. 2021M691728), and the UK Engineering and Physical Sciences Research Council under the project "UK Consortium on Mesoscale Engineering Sciences (UKCOMES)" (Grant No. EP/R029598/1) is gratefully acknowledged. This work made use of computational support by CoSeC, the Computational Science Centre for Research Communities, through UKCOMES. The first author is also grateful for the support of "Shuimu Tsinghua Scholar" program from Tsinghua University.

Supplementary materials

Supplementary material associated with this article can be found, in the online version, at doi:10.1016/j.proci.2022.07.047.

References

[1] Q.L. Yan, F.Q. Zhao, K.K. Kuo, X.H. Zhang, S. Zeman, L.T. DeLuca, Catalytic effects of nano additives on decomposition and combustion of RDX-, HMX-, and AP-based energetic compositions, Prog. Energy Combust. Sci. 57 (2016) 75–136.
[2] W. He, J.H. Guo, C.K. Cao, X.K. Liu, J.Y. Lv, S.W. Chen, P.J. Liu, Q.L. Yan, Catalytic reactivity of graphene oxide stabilized transition metal complexes of triaminoguanidine on thermolysis of RDX, J. Phys. Chem. C 122 (26) (2018) 14714–14724.
[3] T. An, F.Q. Zhao, Q.L. Yan, Y.J. Yang, Y.J. Luo, J.H. Yi, W.L. Hong, Preparation and evaluation of effective combustion catalysts based on Cu(I)/Pb(II) or Cu(II)/Bi(II) nanocomposites carried by graphene oxide (GO), Propellants, Explos. Pyrotech. 43 (11) (2018) 1087–1095.
[4] S. Yuan, Z. Li, Q. Luo, X. Duan, C. Pei, Preparation and thermal decomposition properties of nitrated graphene oxide (NGO)/RDX nano-energetic composites, J. Therm. Anal. Calorim. 139 (3) (2020) 1671–1679.
[5] J. Wang, X. Lian, Q. Yan, D. Gao, F. Zhao, K. Xu, Unusual Cu–Co/GO composite with special high organic content synthesized by an in situ self-assembly approach: pyrolysis and catalytic decomposition on energetic materials, ACS Appl. Mater. Interfaces 12 (25) (2020) 28496–28509.
[6] B. Liu, W. Wang, J. Wang, Y. Zhang, K. Xu, F. Zhao, Preparation and catalytic activities of $CuFe_2O_4$ nanoparticles assembled with graphene oxide for RDX thermal decomposition, J. Nanoparticle Res. 21 (3) (2019) 48.
[7] Y. Zhang, L. Xiao, K. Xu, J. Song, F. Zhao, Graphene oxide-enveloped Bi_2WO_6 composites as a highly efficient catalyst for the thermal decomposition of cyclotrimethylenetrinitramine, RSC Adv 6 (48) (2016) 42428–42434.
[8] Y. Zu, Y. Zhang, K. Xu, F. Zhao, A graphene oxide–$MgWO_4$ nanocomposite as an efficient catalyst for the thermal decomposition of RDX, HMX, RSC Adv 6 (37) (2016) 31046–31052.
[9] W. Wang, B. Liu, K. Xu, Y. Zu, J. Song, F. Zhao, In-situ preparation of $MgFe_2O_4$-GO nanocomposite and its enhanced catalytic reactivity on decomposition of AP and RDX, Ceram. Int. 44 (15) (2018) 19016–19020.
[10] D. Krishnan, F. Kim, J. Luo, R. Cruz-Silva, L.J. Cote, H.D. Jang, J. Huang, Energetic graphene oxide: Challenges and opportunities, Nano Today 7 (2) (2012) 137–152.
[11] T. Senftle, S. Hong, M.M. Islam, S.B. Kylasa, Y. Zheng, Y.K. Shin, C. Junkermeier, R. Engel-Herbert, M.J. Janik, H.M. Aktulga, T. Verstraelen, A. Grama, A.C.T. van Duin, The ReaxFF reactive force-field: development, applications, and future directions, Npj Comput. Mater. 2 (2016) 15011.
[12] C. Ashraf, A.C.T. Van Duin, Extension of the ReaxFF combustion force field toward syngas com-

bustion and initial oxidation kinetics, J. Phys. Chem. A 121 (5) (2017) 1051–1068.
[13] M. Feng, X.Z. Jiang, K.H. Luo, A reactive molecular dynamics simulation study of methane oxidation assisted by platinum/graphene-based catalysts, Proc. Combust. Inst. 37 (2019) 5473–5480.
[14] M. Feng, X.Z. Jiang, Q. Mao, K.H. Luo, P. Hellier, Initiation mechanisms of enhanced pyrolysis and oxidation of JP-10 (exo-tetrahydrodicyclopentadiene) on functionalized graphene sheets: Insights from ReaxFF molecular dynamics simulations, Fuel 254 (2019) 115643.
[15] M. Feng, X.Z. Jiang, W. Zeng, K.H. Luo, P. Hellier, Ethanol oxidation with high water content: A reactive molecular dynamics simulation study, Fuel 235 (2019) 515–521.
[16] X.Z. Jiang, M. Feng, W. Zeng, K.H. Luo, Study of mechanisms for electric field effects on ethanol oxidation via reactive force field molecular dynamics, Proc. Combust. Inst. 37 (2019) 5525–5535.
[17] M. Feng, H. Li, Q. Mao, K.H. Luo, P. Hellier, Fundamental study on mechanisms of thermal decomposition and oxidation of aluminum hydride, J. Phys. Chem. C 123 (40) (2019) 24436–24445.
[18] M. Feng, H. Li, K.H. Luo, A molecular dynamics study on oxidation of aluminum hydride (AlH_3)/hydroxyl-terminated polybutadiene (HTPB) solid fuel, Proc. Combust. Inst. 38 (2021) 4469–4476.
[19] S. Plimpton, Fast parallel algorithms for short-range molecular dynamics, J. Comput. Phys. 117 (1) (1995) 1–19.
[20] L. Liu, Y. Liu, S.V Zybin, H. Sun, W.A. Goddard, ReaxFF-*lg*: Correction of the ReaxFF reactive force field for London dispersion, with applications to the equations of state for energetic materials, J. Phys. Chem. A 115 (40) (2011) 11016–11022.
[21] C. Zhang, X. Fu, J. Li, X. Fan, G. Zhang, Desensitizing effect of graphene oxide on thermolysis mechanisms of 4,4′-azo-1,2,4-triazole studied by reactive molecular dynamics simulations, J. Phys. Chem. A 123 (7) (2019) 1285–1294.
[22] C.Y. Zhang, Y.S. Wen, X.G. Xue, Self-enhanced catalytic activities of functionalized graphene sheets in the combustion of nitromethane: Molecular dynamic simulations by molecular reactive force field, ACS Appl. Mater. Interfaces 6 (15) (2014) 12235–12244.
[23] A. Stukowski, Visualization and analysis of atomistic simulation data with OVITO–the Open Visualization Tool, Model. Simul. Mater. Sci. Eng. 18 (1) (2009) 15012.
[24] V.V Zhurov, E.A. Zhurova, A.I. Stash, A.A. Pinkerton, Importance of the consideration of anharmonic motion in charge-density studies: a comparison of variable-temperature studies on two explosives, RDX and HMX, Acta Crystallogr. Sect. A 67 (2) (2011) 160–173.
[25] W. Li, X. Zheng, Z. Dong, C. Li, W. Wang, Y. Yan, J. Zhang, Molecular dynamics simulations of CO_2/N_2 separation through two-dimensional graphene oxide membranes, J. Phys. Chem. C 120 (45) (2016) 26061–26066.
[26] L.M. Liu, R. Car, A. Selloni, D.M. Dabbs, I.A. Aksay, R.A. Yetter, Enhanced thermal decomposition of nitromethane on functionalized graphene sheets: Ab initio molecular dynamics simulations, J. Am. Chem. Soc. 134 (46) (2012) 19011–19016.
[27] M. Khichar, L. Patidar, S.T. Thynell, Improvement and validation of a detailed reaction mechanism for thermal decomposition of RDX in liquid phase, Combust. Flame 198 (2018) 455–465.
[28] Z. Yan, W. Liu, Y. Jiang, Y. Xie, C. Zhang, J. Wang, G. Zhou, L. Yang, X. Xiang, X. Li, W. Liao, H. Wang, J. Li, B. Tan, M. Huang, Z. Yang, Z. Li, L. Li, M. Li, X. Yuan, et al., Laser initiation of RDX crystal slice under ultraviolet and near-infrared irradiations, Combust. Flame 190 (2018) 112–118.
[29] X. Chen, C.Franklin Goldsmith, Predictive kinetics for the thermal decomposition of RDX, Proc. Combust. Inst. 37 (2019) 3167–3173.
[30] L. Patidar, S.T. Thynell, Quantum mechanics investigation of initial reaction pathways and early ring-opening reactions in thermal decomposition of liquid-phase RDX, Combust. Flame 178 (2017) 7–20.
[31] W. Hao, L. Niu, R. Gou, C. Zhang, Influence of Al and Al_2O_3 nanoparticles on the thermal decay of 1,3,5-trinitro-1,3,5-triazinane (RDX): Reactive molecular dynamics simulations, J. Phys. Chem. C 123 (22) (2019) 14067–14080.
[32] K.L. Joshi, S. Chaudhuri, Reactive simulation of the chemistry behind the condensed-phase ignition of RDX from hot spots, Phys. Chem. Chem. Phys. 17 (28) (2015) 18790–18801.
[33] C.F. Li, Z. Mei, F.Q. Zhao, S.Y. Xu, X.H. Ju, Molecular dynamic simulation for thermal decomposition of RDX with nano-AlH_3 particles, Phys. Chem. Chem. Phys. 20 (20) (2018) 14192–14199.
[34] A. Strachan, E.M. Kober, A.C.T. van Duin, J. Oxgaard, W.A. Goddard, Thermal decomposition of RDX from reactive molecular dynamics, J. Chem. Phys. 122 (5) (2005) 54502.
[35] L. Zhang, SV Zybin, A.C.T. van Duin, S. Dasgupta, W.A. Goddard, E.M. Kober, Carbon cluster formation during thermal decomposition of octahydro-1,3,5,7-tetranitro-1,3,5,7-tetrazocine and 1,3,5-triamino-2,4,6-trinitrobenzene high explosives from ReaxFF reactive molecular dynamics simulations, J. Phys. Chem. A 113 (40) (2009) 10619–10640.
[36] M.Y. Zorainy, W.F. Aly, A. Elbeih, M. Gobara, Preparation and sensitivity measurements of graphene oxide-RDX composite, MATEC Web Conf 136 (2017).
[37] G. Henkelman, B.P. Uberuaga, H. Jónsson, A climbing image nudged elastic band method for finding saddle points and minimum energy paths, J. Chem. Phys. 113 (22) (2000) 9901–9904.
[38] N.J. Harris, K. Lammertsma, Ab initio density functional computations of conformations and bond dissociation energies for hexahydro-1,3,5-trinitro-1,3,5-triazine, J. Am. Chem. Soc. 119 (28) (1997) 6583–6589.

Please cite this article as: M. Feng, Y. Wang and K.H. Luo, Atomistic insight into enhanced thermal decomposition of energetic material on graphene oxide, Proceedings of the Combustion Institute, https://doi.org/10.1016/j.proci.2022.07.047